Atmospheric
Chemistry
and Physics
Discussions

Open Access

10 yr spatial and temporal trends of PM$_{2.5}$ concentrations in the southeastern US estimated using high-resolution satellite data

X. Hu[1], L. A. Waller[2], A. Lyapustin[3], Y. Wang[3,4], and Y. Liu[1]

[1]Department of Environmental Health, Rollins School of Public Health, Emory University, Atlanta, GA 30322, USA
[2]Department of Biostatistics & Bioinformatics, Rollins School of Public Health, Emory University, Atlanta, GA 30322, USA
[3]NASA Goddard Space Flight Center, Greenbelt, Maryland, USA
[4]University of Maryland Baltimore County, Baltimore, Maryland, USA

Correspondence to: Y. Liu (yang.liu@emory.edu)

Abstract

Long-term PM$_{2.5}$ exposure has been reported to be associated with various adverse health outcomes. However, most ground monitors are located in urban areas, leading to a potentially biased representation of the true regional PM$_{2.5}$ levels. To facilitate epidemiological studies, accurate estimates of spatiotemporally continuous distribution of PM$_{2.5}$ concentrations are essential. Satellite-retrieved aerosol optical depth (AOD) has been widely used for PM$_{2.5}$ concentration estimation due to its comprehensive spatial coverage. Nevertheless, an inherent disadvantage of current AOD products is their coarse spatial resolutions. For instance, the spatial resolutions of the Moderate Resolution Imaging Spectroradiometer (MODIS) and the Multiangle Imaging Spectro-Radiometer (MISR) are 10 km and 17.6 km, respectively. In this paper, a new AOD product with 1 km spatial resolution retrieved by the multi-angle implementation of atmospheric correction (MAIAC) algorithm was used. A two-stage model was developed to account for both spatial and temporal variability in the PM$_{2.5}$-AOD relationship by incorporating the MAIAC AOD, meteorological fields, and land use variables as predictors. Our study area is in the southeastern US, centered at the Atlanta Metro area, and data from 2001 to 2010 were collected from various sources. The model was fitted for each year individually, and we obtained model fitting R^2 ranging from 0.71 to 0.85, MPE from 1.73 to 2.50 μg m^{-3}, and RMSPE from 2.75 to 4.10 μg m^{-3}. In addition, we found cross validation R^2 ranging from 0.62 to 0.78, MPE from 2.00 to 3.01 μg m^{-3}, and RMSPE from 3.12 to 5.00 μg m^{-3}, indicating a good agreement between the estimated and observed values. Spatial trends show that high PM$_{2.5}$ levels occurred in urban areas and along major highways, while low concentrations appeared in rural or mountainous areas. A time series analysis was conducted to examine temporal trends of PM$_{2.5}$ concentrations in the study area from 2001 to 2010. The results showed that the PM$_{2.5}$ levels in the study area followed a generally declining trend from 2001 to 2010 and decreased about 20 % during the period. However, there was an exception of an increase in year 2005, which is attributed to elevated sulfate concentrations in the study area in

warm months of 2005. An investigation of the impact of wild and prescribed fires on $PM_{2.5}$ levels in 2007 suggests a positive relationship between them.

1 Introduction

Long-term exposure to $PM_{2.5}$ (particle size less than 2.5 µm in the aerodynamic di-
ameter) is associated with various adverse health outcomes including respiratory and
cardiovascular diseases (Crouse et al., 2012; Peng et al., 2009). Due to the spatiotem-
porally continuous nature of fine particles, obtaining long-term and spatially-resolved
distribution of $PM_{2.5}$ concentrations is important to reduce exposure misclassification
and facilitate accurate epidemiological studies in the region. In addition, time series
analyses of air pollution and human health have become the most common study
design to compare day-to-day fluctuations of air pollution and corresponding fluctu-
ations in health outcomes (Ito et al., 2007), requiring long-term $PM_{2.5}$ concentration
estimates. Previous research examined temporal trends in $PM_{2.5}$ levels. For instance,
Weber et al. (2003) investigated the temporal variations in $PM_{2.5}$ mass at the US En-
vironmental Protection Agency (EPA) Atlanta Supersite Experiment in August 1999.
So et al. (2007) examined long-term variation in $PM_{2.5}$ levels during two 12 month pe-
riods in Hong Kong. EPA (2011) reported temporal trends of annual and 24 h mean
$PM_{2.5}$ concentrations at the national level from 2001 to 2010 and found that annual and
24 h mean $PM_{2.5}$ concentrations dropped 24 % and 28 %, respectively, within these ten
years.

Another critical aspect is the investigation of spatial trends of $PM_{2.5}$ levels. Station-
ary ambient monitors have been established to measure ground-level $PM_{2.5}$ concentra-
tions, yet those point measurements leave large areas uncovered, and therefore spatial
variability is difficult to assess with those point measurements alone. In addition, these
sites do not measure individual-specific exposure, and thus this approach inevitably
introduce measurement errors that likely have substantial implications for interpret-
ing epidemiological studies, especially for time-series analyses (Zeger et al., 2000).

Title Page

Abstract | Introduction

Conclusions | References

Tables | Figures

|◄ | ►|

◄ | ►

Back | Close

Full Screen / Esc

Printer-friendly Version

Interactive Discussion

On the other hand, aerosol observations from satellite remote sensing could substantially improve estimates of population exposure to $PM_{2.5}$ (van Donkelaar et al., 2010). As a result, satellite-retrieved aerosol optical depth (AOD) that measures light extinction by aerosols in the atmospheric column has been widely used to predict ground-level $PM_{2.5}$ concentrations, considering its relatively low cost and large spatiotemporal coverage. A number of AOD products from sensors such as the Moderate Resolution Imaging Spectroradiometer (MODIS), the Multiangle Imaging SpectroRadiometer (MISR), and the Geostationary Operational Environmental Satellite Aerosol/Smoke Product (GASP) have been applied to $PM_{2.5}$ concentration prediction in previous studies (Liu et al., 2007, 2009; Paciorek et al., 2008; Hu et al., 2013). Nevertheless, one of the limitations inherent with those AOD products is their coarse spatial resolutions. For instance, the spatial resolutions of AOD derived from MODIS and MISR are 10 km and 17.6 km, respectively. Although GASP has a spatial resolution of 4 km, the AOD retrievals are less precise than those from the polar-orbiting instruments due to a limited information content (one spectral band) and relatively low signal-to-noise ratio of GOES sensor (Prados et al., 2007). Meanwhile, epidemiological studies typically have access to health data geo-coded to small geographical units (e.g., zip code and census block groups), many of which are substantially smaller than the spatial resolutions of MODIS and MISR. In addition, estimated $PM_{2.5}$ concentrations at coarse resolutions inevitably omit some details of spatial variability of $PM_{2.5}$ exposure and therefore have fundamental limitations in the investigation of spatial trends of $PM_{2.5}$ levels. Hence, it is essential to use high resolution AOD retrievals to generate high spatial resolution $PM_{2.5}$ concentration estimates. Recently, a new AOD product retrieved by a multi-angle implementation of atmospheric correction (MAIAC) algorithm has been reported (Lyapustin et al., 2011b). MAIAC AOD has a spatial resolution of 1 km and thus has the ability to estimate $PM_{2.5}$ concentrations at that resolution. Moreover, the MAIAC AOD has been demonstrated to be strongly associated with monitored $PM_{2.5}$ levels in the New England region (Chudnovsky et al., 2012).
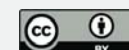
Various statistical methods have been developed to establish the quantitative relationship between $PM_{2.5}$ and satellite-derived AOD including linear regression (Schafer et al., 2008; Wallace et al., 2007; Gupta and Christopher, 2009), many of which do not consider day-to-day variability. Lee et al. (2011) and Kloog et al. (2011) argued that the $PM_{2.5}$-AOD relationship varies day-to-day, and the temporal variability needs to be accounted for in order to improve performance of the AOD-based prediction models. As a result, both studies developed a linear mixed effects model to incorporate daily calibration of the $PM_{2.5}$-AOD relationship and obtained predictions with high accuracy. To move one step further, we introduce a geographically weighted regression (GWR) model as the second stage to account for the spatial variability in the $PM_{2.5}$-AOD relationship.

The objective of this paper is first, to estimate spatiotemporally-resolved $PM_{2.5}$ concentrations in the study domain during the period between 2001 and 2010 using a two-stage model with MAIAC AOD as the primary predictor and meteorological and land use variables as the secondary predictors. Second, maps of annual mean $PM_{2.5}$ concentrations as well as the changes between 2001 and 2010 were generated from the daily estimates to visually illustrate spatial trends of annual $PM_{2.5}$ levels from 2001 to 2010. Third, time series analyses were conducted for the study domain and the Atlanta metro area using the monthly and annual mean $PM_{2.5}$ estimates to examine the 10 yr temporal trends of fine particle levels, and the underlying causes were discussed. Finally, potential impact of wild and prescribed fires on $PM_{2.5}$ levels in the south of our study region was investigated.

2 Materials and methods

2.1 Study area

The study area is approximately $600 \times 600\,km^2$ in the southeastern US, covering most of Georgia, Alabama, and Tennessee, and parts of North and South Carolina (Fig. 1).

The domain includes several large urban centers, numerous medium to small cities, and suburban and rural areas. Additionally, Zhang et al. (2010) reported that biomass burning contributes 13 % to $PM_{2.5}$ mass annually in the southeastern US. Therefore, to investigate the impact of wild and prescribed fires on $PM_{2.5}$ levels, two test sites of the same size (e.g., $18 \times 18 \, km^2$) were selected in the south of the study area. Those two adjacent sites are both located in rural areas and away from any major emission source. One has an accumulated number of 472 fires from 2001 to 2010 (40 fires in 2007), and the other has a total number of 80 fires during the same period of time (8 fires in 2007).

2.2 $PM_{2.5}$ measurements

The 24 h average $PM_{2.5}$ concentrations from 2001 to 2010 collected from US Environmental Protection Agency (EPA) federal reference monitors (FRM) were downloaded from the EPA's Air Quality System Technology Transfer Network (http://www.epa.gov/ttn/airs/airsaqs/). $PM_{2.5}$ concentrations less than $2 \, \mu g \, m^{-3}$ (~0.2–3 % of total data records) were discarded as they are below the established limit of detection (EPA, 2008a).

2.3 Remote sensing data

MAIAC retrieves aerosol parameters over land at 1 km resolution, which was accomplished by using the time series of MODIS measurements and simultaneous processing of a group of pixels in fixed $25 \times 25 \, km^2$ blocks (Lyapustin et al., 2011a, b, 2012). MAIAC uses a sliding window to collect up to 16 days of MODIS radiance observations over the same area and processes them to obtain surface parameters used for aerosol retrievals. To facilitate the time series analysis, MODIS data are initially gridded to a 1 km resolution in a selected projection. For this work, we used MODIS level 1B (calibrated and geometrically corrected) data from Collection 6 re-processing, which

10 yr trend of $PM_{2.5}$ concentrations in the southeastern US

X. Hu et al.

Title Page

Abstract | Introduction

Conclusions | References

Tables | Figures

|◄ | ►|

◄ | ►

Back | Close

Full Screen / Esc

Printer-friendly Version

Interactive Discussion

removed major effects of temporal calibration degradation of Terra and Aqua, a necessary prerequisite for the trend analysis.

Validation showed that the MAIAC and operational Collection 5 MODIS Dark Target AOD have a similar accuracy over dark and vegetated surfaces, but also showed that MAIAC generally improves accuracy over brighter surfaces, including most urban areas (Lyapustin et al., 2011b). MAIAC AOD data from 2001 to 2010 were obtained from NASA Goddard Space Flight Center.

Zhang et al. (2012) found that Terra and Aqua may provide a good estimate of the daily average of AOD, thus the average of Aqua and Terra measurements can be used to predict $PM_{2.5}$ concentrations. In this study, Aqua (overpass at ∼1:30 p.m. LT) and Terra (overpass at ∼10:30 a.m. LT) MAIAC AOD values were first combined to improve spatial coverage. In a common MAIAC pixel, there might be only one MAIAC product from either Aqua or Terra, or both may be present. In the second case, when we combine them, the averaged value represents the mean of the AOD distribution from 10 a.m. to 2 p.m. LT, yet in the first case, AOD as an indicator of $PM_{2.5}$ abundance is biased towards the atmospheric condition either in the morning or early afternoon. To overcome this bias, Lee et al. (2011) defined a simple ratio between averaged Terra and Aqua AOD to estimate the missing AOD value. In this study, we fitted a linear regression to define the relationship between daily mean AOD values of MAIAC-Terra and MAIAC-Aqua. We used this regression to predict the missing AOD value (i.e., predict MAIAC-Terra AOD with the available MAIAC-Aqua AOD, and vice versa), then averaged the observed and the predicted AOD values together. Finally, we set an upper bound of 2.0 for the combined AOD to reduce potential cloud contamination (∼0.05–0.1 % of total data records were excluded).

The fire detection data for the study region were obtained from the US Department of Agriculture (USDA) Forest Service's Remote Sensing Applications Center for 2001 through 2010 (http://activefiremaps.fs.fed.us/gisdata.php?sensor=modis&extent=north america).

Title Page

Abstract | Introduction

Conclusions | References

Tables | Figures

|◄ | ►|

◄ | ►

Back | Close

Full Screen / Esc

Printer-friendly Version

Interactive Discussion

These data are Terra and Aqua MODIS fire and thermal anomalies data from the official NASA MCD14ML product, Collection 5, Version 1.

2.4 Meteorological fields

The meteorological fields provided by the North American Land Data Assimilation System (NLDAS) Phase 2 were downloaded from the NLDAS website (http://ldas.gsfc.nasa.gov/nldas/). The spatial resolution of NLDAS meteorological data is 1/8th-degree (~13 km). Another meteorological dataset used in this study is the North American Regional Reanalysis (NARR). NARR is a long term, consistent, high-resolution climate dataset for North America (Mesinger et al., 2006). The spatial resolution of the NARR dataset is ~32 km. NLDAS provides most of the meteorological fields used in this analysis, including relative humidity, u-wind, and v-wind, while NARR provides another critical parameter: boundary layer height. To generate daytime meteorological fields corresponding to the MODIS overpass times, 3-hourly NARR measurements and hourly NLDAS measurements from 10 a.m. to 4 p.m. standard local time were averaged.

2.5 Land use variables

Elevation data were downloaded from the national elevation dataset (NED) (http://ned.usgs.gov). NED is the seamless elevation dataset covering the contiguous United States and is distributed by the US Geological Survey (USGS). The elevation data are downloaded at a spatial resolution of 1 arcsec (~30 m). The road data were obtained from ESRI StreetMap USA (Environmental Systems Research Institute, Inc., Redland, CA). The road data at level A1 (limited access highway) were extracted. Summed length of road segments were calculated for each $1 \times 1\,km^2$ MAIAC grid cell, and grid cells with no roads were assigned zero. 2001 and 2006 Landsat-derived land cover maps covering the study area with a spatial resolution of 30 m were downloaded from the National Land Cover Database (NLCD) (http://www.epa.gov/mrlc/nlcd-

2001.html). Forest cover maps were generated by assigning one to forest pixels and zero to others. Primary $PM_{2.5}$ emissions (tons per year) were obtained from the 2002, 2005, and 2008 EPA National Emissions Inventory (NEI) facility emissions reports. Grid cells with multiple emission sources were assigned the summed value, and those with no emissions were assigned zero.

2.6 Data integration

All the data were first re-projected to the USA Contiguous Albers Equal Area Conic USGS coordinate system. For model fitting, a $1 \times 1\,km^2$ square buffer was generated for each $PM_{2.5}$ monitor site. Meteorological fields and AOD values were assigned to each $PM_{2.5}$ monitor site using the nearest neighbor approach. Forest cover and elevation were averaged, while road length and point emissions were summed over the $1 \times 1\,km^2$ square buffer. For $PM_{2.5}$ prediction, the same procedure was performed for each $1 \times 1\,km^2$ MAIAC grid cell.

2.7 Model structure

We developed a two-stage spatiotemporal model. The first stage is a linear mixed effects model with day-specific random intercepts and slopes for AOD, meteorological fields to account for the temporally varying relationship between $PM_{2.5}$ and AOD (Eq. 1). The model structure can be expressed as

$$
\begin{aligned}
PM_{2.5,st} = &(b_0 + b_{0,t}) + (b_1 + b_{1,t})AOD_{st} + (b_2 + b_{2,t})\text{Meteorological Fields}_{st} \\
&+ b_3\text{Elevation}_s + b_4\text{Major Roads}_s + b_5\text{Forest Cover}_s \\
&+ b_6\text{Point Emissions}_s + \varepsilon_{st}(b_{0,t}b_{1,t}b_{2,t}) \sim N[(0,0,0), \Psi]
\end{aligned} \tag{1}
$$

where b_i and $b_{i,t}$ (day-specific) are the fixed and random intercept and slopes, respectively; $PM_{2.5,st}$ is the measured ground level $PM_{2.5}$ concentration ($\mu g\,m^{-3}$) at site s in day t; AOD_{st} is the MAIAC AOD value (unitless) at site s in day t; Meteorologi-

25625

cal Fields$_{st}$ is the meteorological parameters at site s in day t and may include Relative Humidity$_{st}$, Boundary Layer Height$_{st}$, Wind Speed$_{st}$, U-Wind$_{st}$, and V-Wind$_{st}$; Relative Humidity$_{st}$ is the relative humidity (%) at site s in day t; Boundary Layer Height$_{st}$ is the boundary layer height (m) at site s in day t; Wind Speed$_{st}$ is the 2 m wind speed (m s^{-1}) at site s in day t; U-Wind$_{st}$ is the east-west component of wind (m s^{-1}) at site s in day t; V-Wind$_{st}$ is the north-south component of wind (m s^{-1}) at site s in day t; Elevation$_s$ is elevation values (m) at site s; Major Roads$_s$ is road length values (m) at site s; Forest Cover$_s$ is forest cover values at site s; Point Emissions$_s$ is point emissions (t yr^{-1}) at site s; and Ψ is an unstructured variance-covariance matrix for the random effects. The fixed effects affect the population mean and represent the average effects on PM$_{2.5}$ concentration estimates for the entire period, while the random effects contribute to the covariance structure and account for the daily variability in associations between dependent and independent variables.

The second stage is a geographically weighted regression (GWR) model that can generate a continuous surface of estimates for each parameter at each location instead of a universal value for all observations. We fitted a monthly GWR model to calibrate the spatial variability within the PM$_{2.5}$-AOD relationship, and the model can be expressed as

$$PM_{2.5}\_resi_{st} = \beta_{0,s} + \beta_{1,s}AOD_{st} + \varepsilon_{st} \qquad (2)$$

where PM$_{2.5}$_resi$_{st}$ denotes the residuals from the stage one model at site s in month t, AOD$_{st}$ is the MAIAC AOD value (unitless) at site s in month t, and $\beta_{0,s}$ and $\beta_{1,s}$ denote the location-specific intercept and slope, respectively.

It should be noted that the model was fitted for each year individually, and therefore the predictors used in the model may vary for different years. The model structures were determined by comparison of performance of models using different predictors to ensure that relatively better prediction accuracy can be achieved. To assess the goodness of fit of the model, various statistical indicators such as the coefficient of determination (R^2), mean prediction error (MPE), and square root of the mean squared

Title Page

Abstract | Introduction

Conclusions | References

Tables | Figures

◀ | ▶

◀ | ▶

Back | Close

Full Screen / Esc

Printer-friendly Version

Interactive Discussion

prediction errors (RMSPE) were calculated between the fitted PM$_{2.5}$ concentrations from the model and the observations. In addition, a 10-fold cross validation (CV) technique was adopted to assess the potential model over-fitting. That is, the model could perform better on the data used to fit the model than unobserved data. The entire model-fitting dataset was randomly split into ten subsets with approximately 10 % of the total data records in each subset. In each round of cross validation, we selected one subset (10 % of the data) as testing samples and used the remaining nine subsets (90 % of the data) to fit the model. Predictions of the held-out subset (10 % of the data) were made from the fitted model. The process was repeated ten times until every subset was tested. Statistical indicators such as R^2, MPE, and RMSPE were calculated between the CV predicted concentrations and the observations. The model over-fitting assessment was conducted by the comparison between CV and model-fitting statistics. A relative accuracy value was also calculated for each year to make validation results comparable among different years.

The daily PM$_{2.5}$ concentrations were estimated using the model for each year individually. The maps of annual mean PM$_{2.5}$ concentrations as well as the changes between 2001 and 2010 for the study domain and the Atlanta metro area were generated using the daily estimates to visually examine spatial trends of PM$_{2.5}$ levels from 2001 to 2010. Moreover, time series analyses were conducted by year and month, respectively to quantitatively investigate the 10 yr temporal trends of fine particle levels in the study domain and the Atlanta metro area. Finally, an examination of the impact of wild and prescribed fires on PM$_{2.5}$ levels was also conducted on two test sites.

3 Results

3.1 Descriptive statistics

The descriptive statistics of variables used in fitting the models are listed in Table 1. The annual mean PM$_{2.5}$ concentrations ranged from 11.03 to 15.63 µg m^{-3} between

2001 and 2010, the highest occurred in 2005, and the lowest appeared in 2009. The annual mean AOD values ranged from 0.20 to 0.28 during the same period of time. Table 1 also shows that land use variables and meteorological fields vary from year to year within the data.

3.2 Results of model-fitting and validation

The model-fitting and CV statistics (e.g. R^2, MPE, and RMSPE) are listed in Table 2. The results show that R^2 ranges from 0.71 to 0.85, MPE is from 1.73 to 2.50 $\mu g\,m^{-3}$, RMSPE ranges from 2.75 to 4.10 $\mu g\,m^{-3}$, and relative accuracy ranges from 72.9 % to 80.7 %, which indicate a good fit between predicted values from the fitted models and the observations. In addition, CV statistics results suggest that model over-fitting is present; that is, R^2 decreases, while MPE and RMSPE increase from model fitting to cross validation, yet the differences are relatively small for all the years. For instance, R^2 and relative accuracy have an average decrease of 0.08 and 4.21 %, respectively, while MPE and RMSPE have an average increase of 0.39 and 0.60 $\mu g\,m^{-3}$, respectively through all the years. Moreover, a regression with zero intercept (Fig. 2) was performed to fit the predicted values against the observations. The figure shows that at high concentration levels, both model fitting and cross validation under-predicted the $PM_{2.5}$ concentrations by 3–7 % (e.g. fitted/CV $PM_{2.5} = 97$ % to 93 % observed $PM_{2.5}$).

3.3 Spatial trends of $PM_{2.5}$ concentrations

Figure 3 illustrates the $PM_{2.5}$ concentration estimates at 1 km spatial resolution in the study area. The annual mean estimated concentrations are 13.97, 13.90, 13.35, 13.31, 15.19, 13.73, 13.22, 11.34, 10.58, and 11.22 $\mu g\,m^{-3}$ for year 2001 though 2010, respectively. The patterns of $PM_{2.5}$ distribution are very similar for all the years. High concentrations appear in large urban centers and along major highways, while low concentrations occur in rural and mountainous areas. In addition, high $PM_{2.5}$ levels also occur in the south of the study domain. This area is primarily occupied by agriculture

10 yr trend of $PM_{2.5}$ concentrations in the southeastern US

X. Hu et al.

Title Page

Abstract | Introduction

Conclusions | References

Tables | Figures

|◄ | ►|

◄ | ►

Back | Close

Full Screen / Esc

Printer-friendly Version

Interactive Discussion

land, and high agricultural emissions may lead to high concentrations of fine particles. As reported by previous studies, ammonia (NH_3) and nitrogen oxides (NO_x) generated by agricultural activities, such as farm vehicles, domestic and farm animals, and fertilizer applications, can significantly increase the number of suspended particles (Kurvits and Marta, 1998). In addition, biomass burning also contributes to emissions of fine particles in the region (Zhang et al., 2010). Figure 4 shows that the pattern of ground $PM_{2.5}$ measurements from FRM monitors corresponds well with that of our estimated concentrations.

To take advantage of the high spatial resolution of the MAIAC data, a map of $PM_{2.5}$ estimates in Atlanta metro area was also generated for each year (Fig. 5). The annual mean estimates from 2001 to 2010 are 15.10, 14.64, 14.00, 14.54, 15.63, 14.39, 14.14, 11.78, 10.98, and 11.65 $\mu g\,m^{-3}$, respectively. Those maps distinctly show that high $PM_{2.5}$ levels occur in areas with high urban land use and along major highways, while low concentrations appear in forest and recreational areas, suggesting an underlying positive relationship between air pollution levels and urban development.

Figure 6 shows the percent changes in $PM_{2.5}$ concentrations from 2001 to 2010. Figure 6a illustrates the spatial trend of changes in $PM_{2.5}$ levels in the study region. The results show that $PM_{2.5}$ levels in most of the areas decreased from 0 to 25 %, and large parts of the areas had decreases exceeding 25 % and up to 50 %. Larger decreases occurred in areas with generally higher pollution levels such as Atlanta metro area and along major highways, which might be due to recently enacted emission reduction program (EPA, 2011), since majority of the emission sources are located in or near urban areas and along major highways. Mitigation of fine particles has been effected through control of direct $PM_{2.5}$ emissions from both stationary and mobile sources (e.g., through installation of scrubbers and filters and the use of alternative fuels and electric vehicles) (EPA, 2007). One exception is the mountainous area in the northeast of our domain with generally low $PM_{2.5}$ levels. The decreases of $PM_{2.5}$ concentrations in this region from 2001 to 2010 were also phenomenal, $PM_{2.5}$ levels decreased from 25 % to 50 % in most of the region, and some areas had decreases exceeding 50 %.

Title Page

Abstract | Introduction

Conclusions | References

Tables | Figures

|◄ | ►|

◄ | ►

Back | Close

Full Screen / Esc

Printer-friendly Version

Interactive Discussion

By checking 2002 and 2008 EPA NEI facility emissions reports, this is probably due to dramatically reduced number of emission sources in the region during the period. Figure 6b illustrates the percent changes in $PM_{2.5}$ levels in the Atlanta Metro area. Once again, the spatial trend shows that larger decreases (25 % to 50 %) primarily occurred in urban built-up areas and along major highways, while small decreases (0 to 25 %) appeared in forest or recreational areas with generally lower pollution levels. It is reasonable because the increase or decrease of emissions from emission sources might be the major driver causing fluctuations of $PM_{2.5}$ levels in this region, while most of those sources are unlikely to be located in forest and recreational areas. Two pixels with large changes (increasing more than 25 % and decreasing more than 50 %) were identified (in blue and red circles). The large decrease of $PM_{2.5}$ concentration in the blue pixel was because of the large reduction of particle emissions from power plants located within that pixel during the period between 2001 and 2010. Likewise, the large increase of $PM_{2.5}$ concentration in the red pixel was due to the addition of one emission source that did not exist in year 2001.

3.4 Temporal trends of $PM_{2.5}$ concentrations

A time series analysis was conducted to quantitatively examine temporal trends of $PM_{2.5}$ levels in the study area as well as the Atlanta metro area during the period between 2001 and 2010 (Fig. 7). The results show that the estimated $PM_{2.5}$ concentrations are smaller than the monitored observations, and underestimation by our model has occurred, especially in areas with high pollution levels (e.g., the Atlanta metro area), which agrees with our model validation results. The average underestimation is $0.99\,\mu g\,m^{-3}$ for the study domain and $1.82\,\mu g\,m^{-3}$ for the Atlanta metro area. The $PM_{2.5}$ levels in the study region as well as the Atlanta metro area followed a generally declining trend, especially after year 2005. From 2001 to 2010, the annual mean $PM_{2.5}$ concentration decreased about 20 % in the study area and 23 % in the Atlanta metro area, which is in line with the findings documented in the US EPA report on particle pollution (EPA, 2011). Both EPA's and our results illustrate a peak of $PM_{2.5}$ levels in

Title Page

Abstract | Introduction

Conclusions | References

Tables | Figures

|◄ | ►|

◄ | ►

Back | Close

Full Screen / Esc

Printer-friendly Version

Interactive Discussion

year 2005, and this phenomenon might be attributed to the increase of sulfate concentrations emitted from electric utilities and industrial boilers during the warm months (e.g, from May to September) of 2005 (EPA, 2008b). In addition, the steady decrease of $PM_{2.5}$ levels after year 2005 is due to the emissions reduction programs that have been enacted recently (EPA, 2011, 2007).

3.5 The impact of wild and prescribed fires on $PM_{2.5}$ concentrations

Zeng et al. (2008) suggested that prescribed fire emissions can result in a daily increase of $PM_{2.5}$ mass up to $25\,\mu g\,m^{-3}$, indicating high impact of fires on $PM_{2.5}$ levels. Figure 8 illustrates the seasonal distribution of the number of fires in the study region, which shows that most wild and prescribed fires occurred in spring and fall, and the highest number of fires appeared in spring 2007. To assess the impact of fires on $PM_{2.5}$ levels, we selected year 2007 to conduct a case study as fires in the southeastern US in 2007 has been examined by previous research using ground monitoring data (Zhang et al., 2010). The differences of number of fires and annual mean $PM_{2.5}$ concentrations between two test sites were calculated and illustrated in Fig. 9. It shows that in most of the cases, the peaks and valleys of the differences of number of fires correspond well with the peaks and valleys of the differences of $PM_{2.5}$ concentrations (indicated by black arrows), indicating an underlying positive relationship between fires and $PM_{2.5}$ concentrations and suggesting that the fires may have impact on fine particle levels in the south of our study region. However, exceptions exist. For example, in April 2007, a day in which a large difference of number of fires occurred did not show a higher difference of $PM_{2.5}$ concentrations than its neighboring days. In addition, in many days in which there are no differences of number of fires, the differences of $PM_{2.5}$ concentrations between two test sites still exist. Such situations might be attributed to several factors: first, due to the lack of data, our analysis only used the number of fires without fire scale and intensity information and thus might be biased. Second, although the contributions of fires to $PM_{2.5}$ levels are quite significant (~13 % annually) and vary by seasons in the southeastern US, fires might not be major drivers and there are other,

Title Page

Abstract | Introduction

Conclusions | References

Tables | Figures

|◄ | ►|

◄ | ►

Back | Close

Full Screen / Esc

Printer-friendly Version

Interactive Discussion

often more substantial, contributors to $PM_{2.5}$ concentrations in the region (Zhang et al., 2010).

4 Discussion

A major strength of this study is that we used 1 km spatial resolution $PM_{2.5}$ estimates derived from 1 km resolution MAIAC AOD to investigate spatiotemporal trends of $PM_{2.5}$ concentrations in the study area as well as in the Atlanta metro area. $PM_{2.5}$ estimates at finer resolutions are more suitable for investigation of spatial trends than those at coarser resolutions derived from other AOD products (e.g., MODIS and MISR), because estimates at coarser scales inevitably omit local spatial details. Our results are capable of showing $PM_{2.5}$ concentrations and changes within a $1 \times 1\,km^2$ area, which are very useful for air pollution studies at local scales. For instance, spatial trends of changes in $PM_{2.5}$ concentrations in the Atlanta metro area show distinct patterns of higher $PM_{2.5}$ reduction in areas with generally higher pollution levels (e.g., urban built-up areas and along major highways). Some of the changes may be directly associated with the occurrence or disappearance of one or more emission sources as well as the increase or decrease of emissions from those sources. Although high resolution $PM_{2.5}$ estimates can provide more details to examine spatial trends, difficulties lie in validation to ground monitoring. More ground measurements at specific locations are needed to further validate the results.

Our results of temporal trends of $PM_{2.5}$ concentrations correspond well with EPA's results (EPA, 2011). However, results also show that our predicted $PM_{2.5}$ concentrations underestimated the ground measurements for almost all the years, which is expected. Most of the EPA FRM monitors are located in or near urban areas with generally high $PM_{2.5}$ levels. On the other hand, the temporal trends of $PM_{2.5}$ concentrations estimated from satellite AOD include the entire study domain and account for both urban and rural estimates, and therefore might more thoroughly represent the true fluctuations of

Title Page

Abstract | Introduction

Conclusions | References

Tables | Figures

|◄ | ►|

◄ | ►

Back | Close

Full Screen / Esc

Printer-friendly Version

Interactive Discussion

regional fine particle levels, and further research will continue to explore these associations.

In addition, long-term PM$_{2.5}$ estimates at high spatial resolutions might be better suited for incorporating fire data in order to examine the impact of fires on fine particle levels, since fires might occur far away from ground monitors. Our results show that fires, to some extent, contribute to PM$_{2.5}$ concentrations in our study region. However, they might not be the major contributors to fine particle levels. It should be noted that our results are preliminary and might contain a certain degree of bias, since no fire scale and intensity data were incorporated in the analysis. However, in this paper, we primarily attempt to examine the 10 yr spatial and temporal trends of fine particle levels in the region using high spatial resolution PM$_{2.5}$ estimates as well as the possible causes for high PM$_{2.5}$ concentrations in the south of our domain. Hence, quantification of the contribution of fires to PM$_{2.5}$ levels was beyond the scope of this analysis.

5   Conclusions

In this paper, we used a two-stage spatiotemporal model incorporating MAIAC AOD data, meteorological fields, and land use variables to estimate PM$_{2.5}$ concentrations at 1 km spatial resolution and investigated the 10 yr spatial and temporal trends of PM$_{2.5}$ levels in our study region. The results show a reasonable spatial pattern of PM$_{2.5}$ levels in the study area as well as in the Atlanta metro area. For instance, high concentrations occur in large urban centers and along major highways, while low concentrations appear in rural and mountainous area. PM$_{2.5}$ estimates at high spatial resolutions can provide more details in small geographic regions and reduce exposure misclassification in air pollution and epidemiological studies. The spatial trends of changes in PM$_{2.5}$ concentrations indicate that higher pollution reduction occurred in areas with generally higher PM$_{2.5}$ levels (e.g. in urban areas and along major highways), while areas with generally lower pollution levels (e.g., in forest and recreational areas) had lower and moderate reduction of fine particle concentrations.

Our time series analysis results indicate that the PM$_{2.5}$ levels decreased about 20 % in the study region and 23 % in the Atlanta Metro area during the period between 2001 and 2010, especially after year 2005. In addition, an analysis of the impact of wild and prescribed fires on PM$_{2.5}$ concentrations shows that the peaks and valleys of the differences of the number of fires corresponds well with the peaks and valleys of the differences of PM$_{2.5}$ levels between two test sites, suggesting a positive relationship between fires and fine particle exposure that merits further investigation.

References

Chudnovsky, A. A., Kostinski, A., Lyapustin, A., and Koutrakis, P.: Spatial scales of pollution from variable resolution satellite imaging, Environ. Pollut., 172, 131–138, doi:10.1016/j.envpol.2012.08.016, 2012.

Crouse, D. L., Peters, P. A., van Donkelaar, A., Goldberg, M. S., Villeneuve, P. J., Brion, O., Khan, S., Atari, D. O., Jerrett, M., Pope, C. A., Brauer, M., Brook, J. R., Martin, R. V., Stieb, D., and Burnett, R. T.: Risk of non accidental and cardiovascular mortality in relation to long-term exposure to low concentrations of fine particulate matter: a Canadian National-Level Cohort study, Environ. Health Persp., 120, 708–714, doi:10.1289/ehp.1104049, 2012.

Gupta, P. and Christopher, S. A.: Particulate matter air quality assessment using integrated surface, satellite, and meteorological products: Multiple regression approach, J. Geophys. Res.-Atmos., 114, D14205, doi10.1029/2008jd011496, 2009.

Hu, X., Waller, L. A., Al-Hamdan, M. Z., Crosson, W. L., Estes Jr, M. G., Estes, S. M., Quattrochi, D. A., Sarnat, J. A., and Liu, Y.: Estimating ground-level PM$_{2.5}$ concentrations in the southeastern U.S. using geographically weighted regression, Environ. Res., 121, 1–10, doi:10.1016/j.envres.2012.11.003, 2013.

Title Page

Abstract | Introduction

Conclusions | References

Tables | Figures

Back | Close

Full Screen / Esc

Printer-friendly Version

Interactive Discussion

Ito, K., Thurston, G. D., and Silverman, R. A.: Characterization of $PM_{2.5}$, gaseous pollutants, and meteorological interactions in the context of time-series health effects models, J. Expo. Sci. Env. Epid., 17, S45–S60, 2007.

Kurvits, T. and Marta, T.: Agricultural NH_3 and NO_x emissions in Canada, Environ. Pollut., 102, 187–194, doi:10.1016/S0269-7491(98)80032-8, 1998.

Lee, H. J., Liu, Y., Coull, B. A., Schwartz, J., and Koutrakis, P.: A novel calibration approach of MODIS AOD data to predict $PM_{2.5}$ concentrations, Atmos. Chem. Phys., 11, 7991–8002, doi:10.5194/acp-11-7991-2011, 2011.

Liu, Y., Franklin, M., Kahn, R., and Koutrakis, P.: Using aerosol optical thickness to predict ground-level $PM_{2.5}$ concentrations in the St. Louis area: a comparison between MISR and MODIS, Remote Sens. Environ., 107, 33–44, doi:10.1016/j.rse.2006.05.022, 2007.

Liu, Y., Paciorek, C. J., and Koutrakis, P.: Estimating regional spatial and temporal variability of $PM_{2.5}$ concentrations using satellite data, meteorology, and land use information, Environ. Health Persp., 117, 886–892, 2009.

Lyapustin, A., Martonchik, J., Wang, Y. J., Laszlo, I., and Korkin, S.: Multiangle implementation of atmospheric correction (MAIAC): 1. Radiative transfer basis and look-up tables, J. Geophys. Res.-Atmos., 116, D03210, doi:10.1029/2010jd014985, 2011a.

Lyapustin, A., Wang, Y., Laszlo, I., Kahn, R., Korkin, S., Remer, L., Levy, R., and Reid, J. S.: Multiangle implementation of atmospheric correction (MAIAC): 2. Aerosol algorithm, J. Geophys. Res.-Atmos., 116, D03211, doi:10.1029/2010jd014986, 2011b.

Lyapustin, A. I., Wang, Y., Laszlo, I., Hilker, T., Hall, F. G., Sellers, P. J., Tucker, C. J., and Korkin, S. V.: Multi-angle implementation of atmospheric correction for MODIS (MAIAC): 3. Atmospheric correction, Remote Sens. Environ., 127, 385–393, doi:10.1016/j.rse.2012.09.002, 2012.

Mesinger, F., DiMego, G., Kalnay, E., Mitchell, K., Shafran, P. C., Ebisuzaki, W., Jovic, D., Woollen, J., Rogers, E., and Berbery, E. H.: North American regional reanalysis, B. Am. Meteorol. Soc., 87, 343–360, 2006.

Paciorek, C. J., Liu, Y., Moreno-Macias, H., and Kondragunta, S.: Spatiotemporal associations between GOES aerosol optical depth retrievals and ground-level $PM_{2.5}$, Environ. Sci. Technol., 42, 5800–5806, doi:10.1021/es703181j, 2008.

Peng, R. D., Bell, M. L., Geyh, A. S., McDermott, A., Zeger, S. L., Samet, J. M., and Dominici, F.: Emergency admissions for cardiovascular and respiratory diseases and the

Title Page

Abstract | Introduction

Conclusions | References

Tables | Figures

|◄ | ►|

◄ | ►

Back | Close

Full Screen / Esc

Printer-friendly Version

Interactive Discussion

chemical composition of fine particle air pollution, Environ. Health Persp., 117, 957–963, doi:10.1289/ehp.0800185, 2009.

Prados, A. I., Kondragunta, S., Ciren, P., and Knapp, K. R.: GOES Aerosol/Smoke Product (GASP) over North America: comparisons to AERONET and MODIS observations, J. Geophys. Res., 112, D15201, doi:10.1029/2006jd007968, 2007.

Schafer, K., Harbusch, A., Emeis, S., Koepke, P., and Wiegner, M.: Correlation of aerosol mass near the ground with aerosol optical depth during two seasons in Munich, Atmos. Environ., 42, 4036–4046, doi:10.1016/j.atmosenv.2008.01.060, 2008.

So, K. L., Guo, H., and Li, Y. S.: Long-term variation of $PM_{2.5}$ levels and composition at rural, urban, and roadside sites in Hong Kong: increasing impact of regional air pollution, Atmos. Environ., 41, 9427–9434, doi:10.1016/j.atmosenv.2007.08.053, 2007.

van Donkelaar, A., Martin, R. V., Brauer, M., Kahn, R., Levy, R., Verduzco, C., and Villeneuve, P. J.: Global estimates of ambient fine particulate matter concentrations from satellite-based aerosol optical depth: development and application, Environ. Health Persp., 118, 847–855, doi:10.1289/ehp.0901623, 2010.

Wallace, J., Kanaroglou, P., and Ieee: An investigation of air pollution in southern Ontario, Canada, with MODIS and MISR aerosol data, in: Igarss: 2007 Ieee International Geoscience and Remote Sensing Symposium, Vol. 1–12 – Sensing and Understanding Our Planet, IEEE International Symposium on Geoscience and Remote Sensing (IGARSS), Ieee, New York, July 23–28, 4311–4314, 2007.

Weber, R., Orsini, D., Duan, Y., Baumann, K., Kiang, C. S., Chameides, W., Lee, Y. N., Brechtel, F., Klotz, P., Jongejan, P., ten Brink, H., Slanina, J., Boring, C. B., Genfa, Z., Dasgupta, P., Hering, S., Stolzenburg, M., Dutcher, D. D., Edgerton, E., Hartsell, B., Solomon, P., and Tanner, R.: Intercomparison of near real time monitors of $PM_{2.5}$ nitrate and sulfate at the US Environmental Protection Agency Atlanta Supersite, J. Geophys. Res.-Atmos., 108, 8421, doi:10.1029/2001jd001220, 2003.

Zeger, S. L., Thomas, D., Dominici, F., Samet, J. M., Schwartz, J., Dockery, D., and Cohen, A.: Exposure measurement error in time-series studies of air pollution: concepts and consequences, Environ. Health Persp., 108, 419–426, doi:10.2307/3454382, 2000.

Zeng, T., Wang, Y., Yoshida, Y., Tian, D., Russell, A. G., and Barnard, W. R.: Impacts of prescribed fires on air quality over the southeastern United States in spring based on modeling and ground/satellite measurements, Environ. Sci. Technol., 42, 8401–8406, doi:10.1021/es800363d, 2008.

Title Page

Abstract | Introduction

Conclusions | References

Tables | Figures

◄◄ | ►►

◄ | ►

Back | Close

Full Screen / Esc

Printer-friendly Version

Interactive Discussion

Zhang, X., Hecobian, A., Zheng, M., Frank, N. H., and Weber, R. J.: Biomass burning impact on $PM_{2.5}$ over the southeastern US during 2007: integrating chemically speciated FRM filter measurements, MODIS fire counts and PMF analysis, Atmos. Chem. Phys., 10, 6839–6853, doi:10.5194/acp-10-6839-2010, 2010.

5 Zhang, Y., Yu, H., Eck, T. F., Smirnov, A., Chin, M., Remer, L. A., Bian, H., Tan, Q., Levy, R., Holben, B. N., and Piazzolla, S.: Aerosol daytime variations over North and South America derived from multiyear AERONET measurements, J. Geophys. Res.-Atmos., 117, D05211, doi:10.1029/2011jd017242, 2012.

Title Page	
Abstract	Introduction
Conclusions	References
Tables	Figures

◄	►|
◄	►
Back	Close

Full Screen / Esc

Printer-friendly Version

Interactive Discussion

Table 1. Descriptive statistics (2001–2010).

Var.	Min	Std. dev.	Max	Mean
PM$_{2.5}$ (μg m^{-3})	2.0–2.6	5.31–8.64	50.1–145.0	11.03–15.63
Boundary layer height (m)	215–464	347–493	2605–3405	1146–1464
Relative humidity (%)	13.9–26.2	8.7–11.3	86.8–93.1	46.8–59.9
U-wind (m s^{-1})	−9.44 to −6.30	2.62–3.20	10.22–16.85	0.82–1.47
V-wind (m s^{-1})	−12.60 to −9.34	2.62–3.00	8.45–11.84	−0.74 to −0.09
Wind speed (m s^{-1})	0.03–0.12	1.81–2.13	12.76–18.06	3.48–3.99
Forest cover 2001	0	0.16–0.18	0.83	0.14–0.17
Forest cover 2006	0	0.15–0.17	0.79	0.14–0.16
Road length (m)	0	187.29–230.81	1012.97–1078.09	58.05–82.92
Elevation (m)	46.78	126.82–141.65	811.63–822.82	227.74–249.10
Point emissions 2002 (t yr^{-1})	0	56.64–70.39	364.42	11.13–16.46
Point emissions 2005 (t yr^{-1})	0	150.89–188.63	985.48	26.90–40.84
Point emissions 2008 (t yr^{-1})	0	15.89–19.72	101.74	3.14–4.54
AOD	0–0.01	0.16–0.26	1.42–1.96	0.20–0.28

Table 2. Model validation.

Year	Model fitting				Cross validation			
	R^2	MPE ($\mu g\,m^{-3}$)	RMSPE ($\mu g\,m^{-3}$)	Relative accuracy (%)[a]	R^2	MPE ($\mu g\,m^{-3}$)	RMSPE ($\mu g\,m^{-3}$)	Relative accuracy (%)[a]
2001	0.78	2.50	4.10	72.9	0.67	3.01	5.00	67.0
2002	0.84	2.10	2.98	80.7	0.75	2.62	3.75	75.7
2003	0.85	1.95	2.77	80.4	0.76	2.42	3.47	75.4
2004	0.85	1.97	2.77	80.3	0.77	2.40	3.37	76.1
2005	0.84	2.23	3.17	79.7	0.78	2.64	3.76	75.9
2006	0.85	2.02	2.90	80.6	0.78	2.43	3.49	76.6
2007	0.79	2.26	3.75	74.0	0.71	2.64	4.39	69.6
2008	0.74	1.93	3.13	75.4	0.67	2.21	3.53	72.3
2009	0.71	1.73	2.88	73.9	0.62	2.00	3.28	70.3
2010	0.73	1.90	2.75	77.6	0.66	2.15	3.12	74.5

[a] Relative accuracy is defined as 100 % − RMSPE/the mean PM$_{2.5}$ concentration.
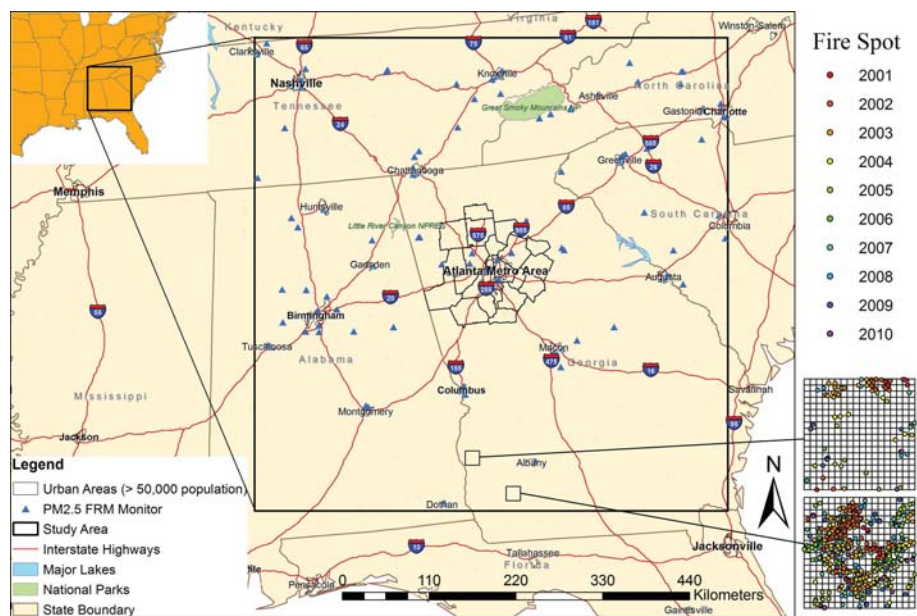
Fig. 1. Study area and two test sites.

Title Page

Abstract | Introduction

Conclusions | References

Tables | Figures

◄ | ►

◄ | ►

Back | Close

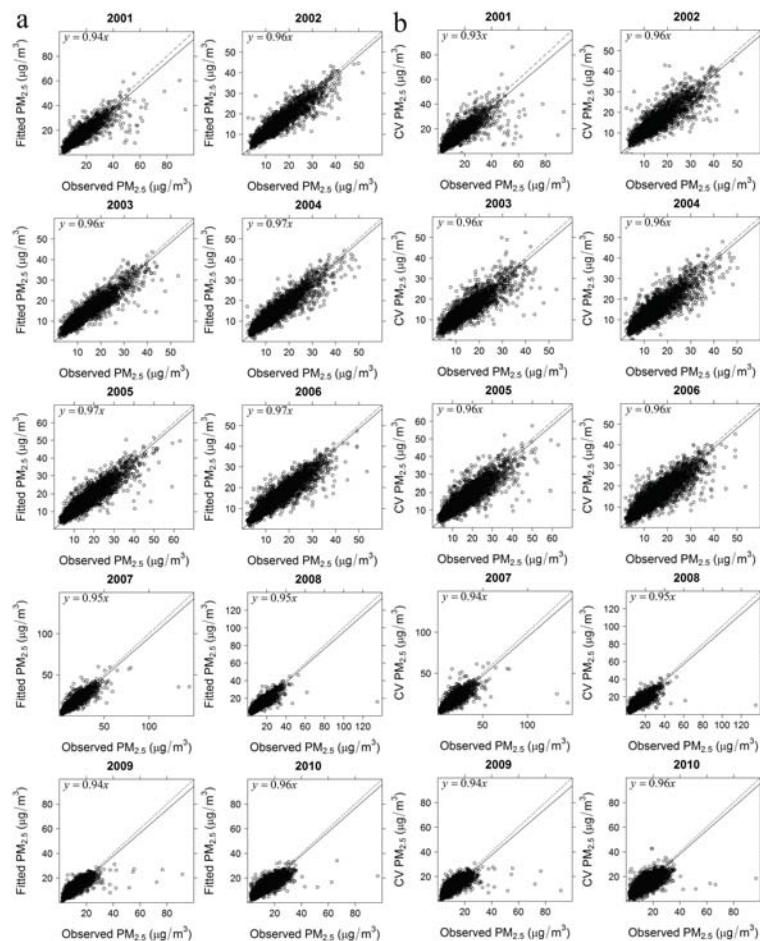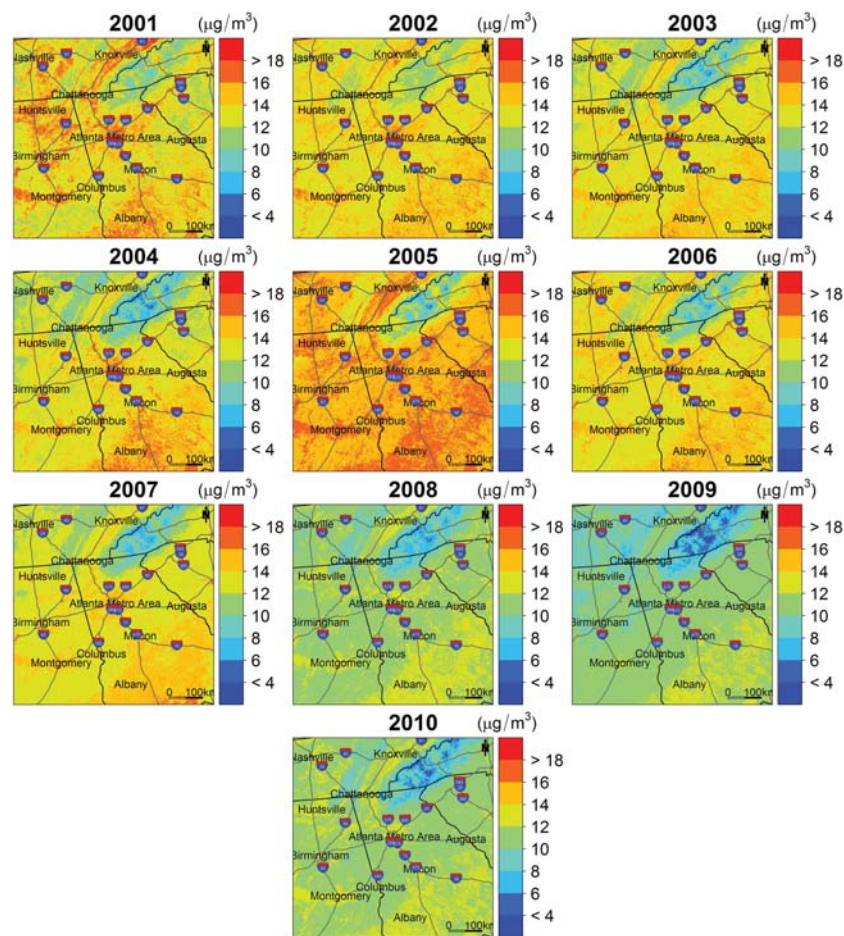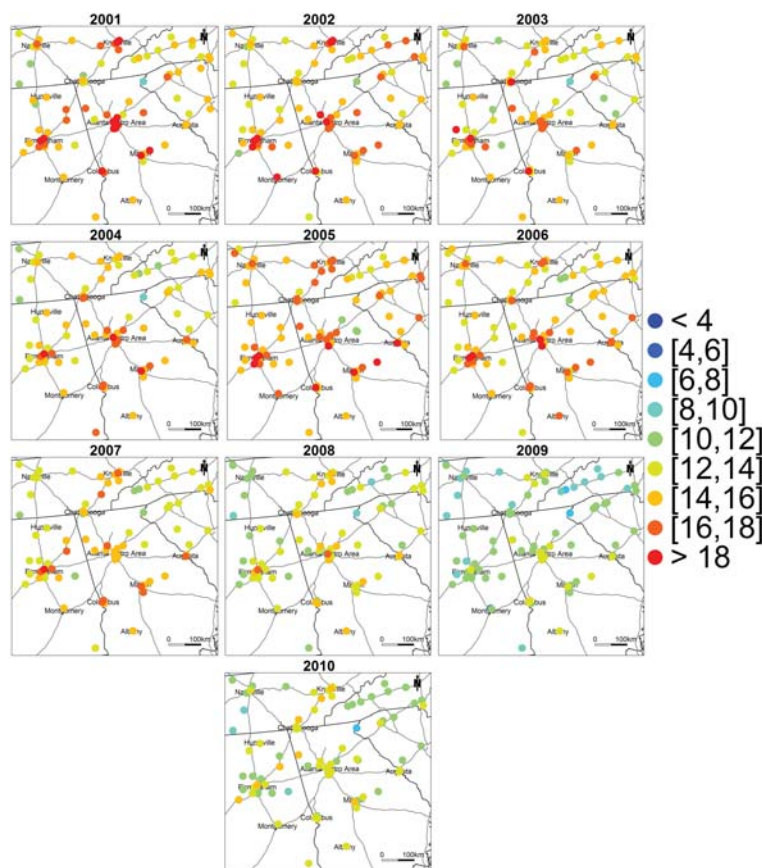Full Screen / Esc

Printer-friendly Version

Interactive Discussion

Fig. 2. Model validation. **(a)** Model fitting; **(b)** cross validation.

Title Page

Abstract | Introduction

Conclusions | References

Tables | Figures

|◄ | ►|

◄ | ►

Back | Close

Full Screen / Esc

Printer-friendly Version

Interactive Discussion

Fig. 3. Annual mean PM$_{2.5}$ concentration predictions in the study area.

Full Screen / Esc

Printer-friendly Version

Interactive Discussion

Fig. 4. Annual mean PM$_{2.5}$ concentration measured from ground FRM monitors.

Title Page

Abstract | Introduction

Conclusions | References

Tables | Figures

|◀ | ▶|

◀ | ▶

Back | Close

Full Screen / Esc

Printer-friendly Version
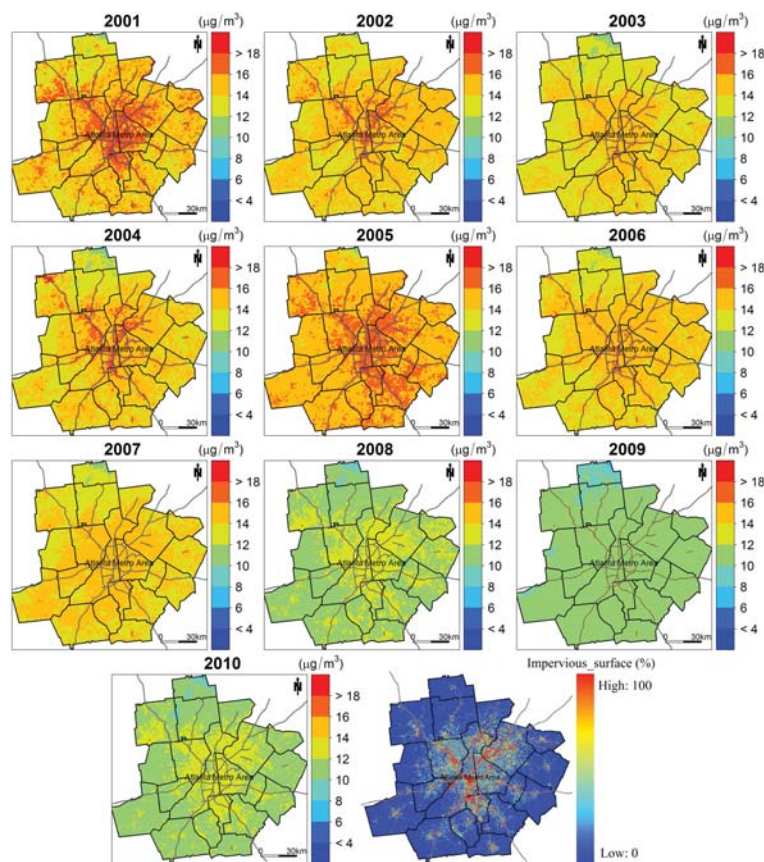
Interactive Discussion

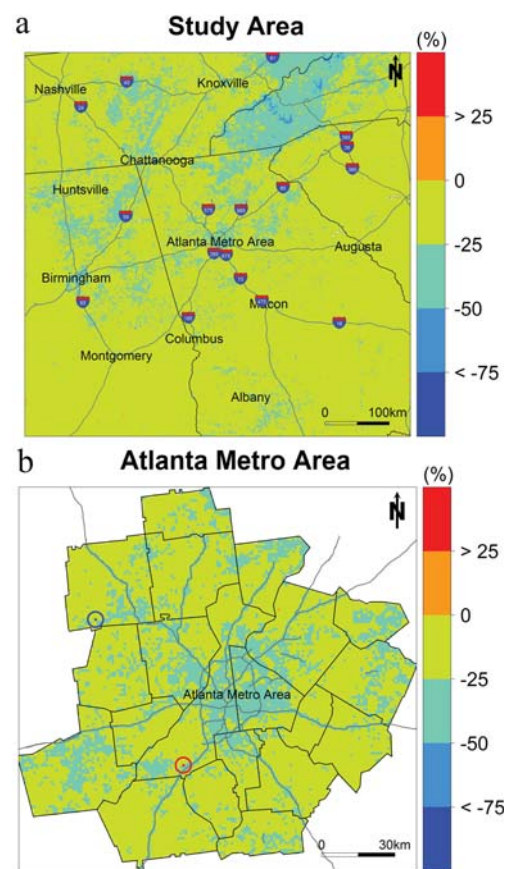**Fig. 5.** Annual mean PM$_{2.5}$ concentration predictions in the Atlanta metro area.

Title Page

Abstract | Introduction

Conclusions | References

Tables | Figures

|◀ | ▶|

◀ | ▶

Back | Close

Full Screen / Esc

Printer-friendly Version

Interactive Discussion

Fig. 6. The percent change of PM$_{2.5}$ concentrations in the study area **(a)** and the Atlanta metro area **(b)** from 2001 to 2010.
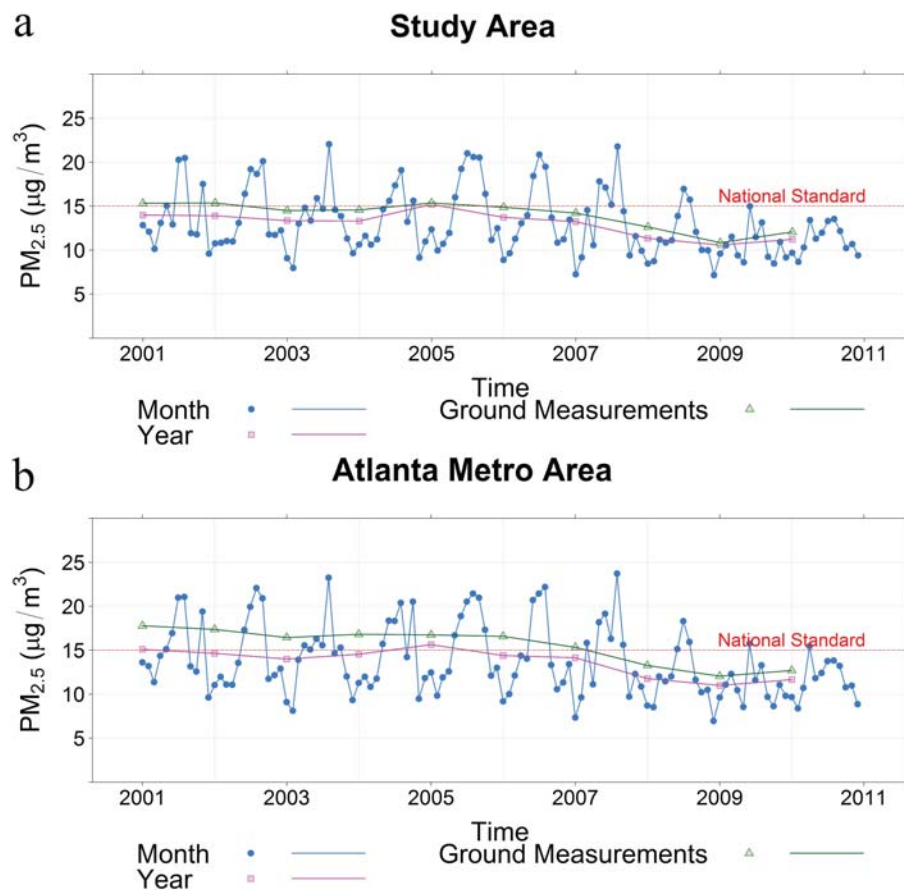
Fig. 7. Time series analysis of annual and monthly PM$_{2.5}$ concentrations. **(a)** Study area; **(b)** Atlanta metro area.
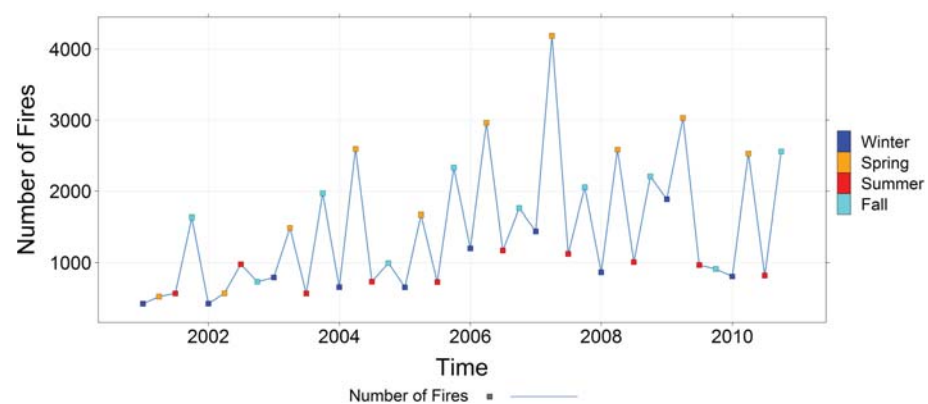
Fig. 8. Time series analysis of number of fires that occurred in the study area from 2001 to 2010.
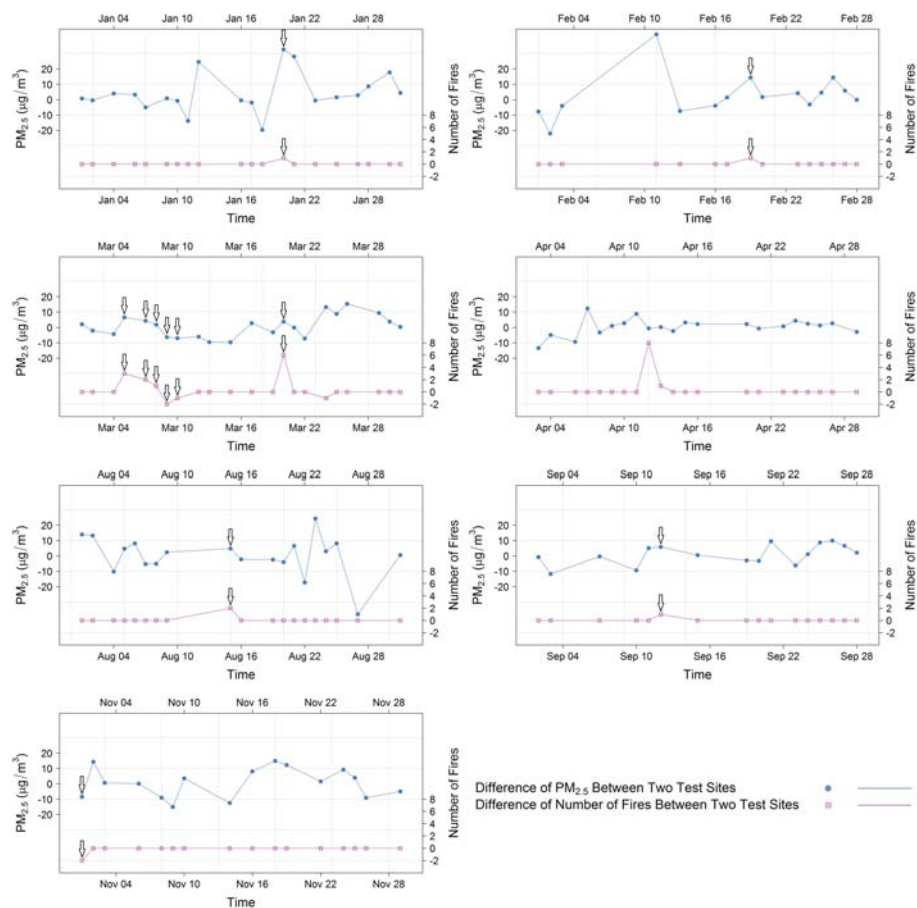
Fig. 9. Time series analysis of relationship between differences of number of fires and differences of PM$_{2.5}$ concentrations for year 2007 (Only months with differences of number of fires were plotted, and the coincidences were indicated by black arrows).

Title Page

Abstract | Introduction

Conclusions | References

Tables | Figures

|◀ | ▶|

◀ | ▶

Back | Close

Full Screen / Esc

Printer-friendly Version

Interactive Discussion